POLITECNICO
MILANO 1863

DIPARTIMENTO DI MECCANICA

mecc

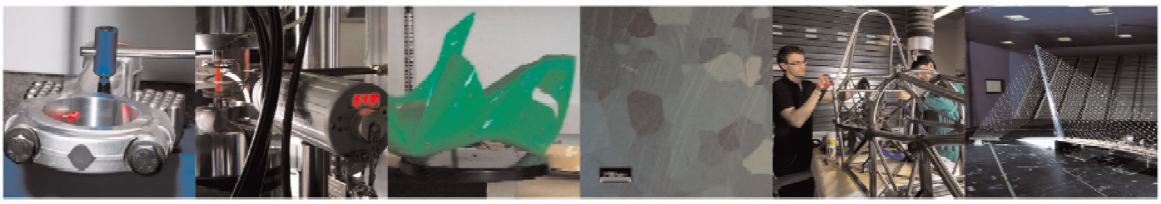

Experimental characterization of the vibration effects on wheels of a mass rapid transit vehicle

Luigi Calvanese, Egidio Di Gialleonardo & Marco Bocciolone

This is a post-peer-review, pre-copyedit version of an article published in Proceedings of the Institution of Mechanical Engineers, Part F: Journal of Rail and Rapid Transit. The final authenticated version is available online at: http://dx.doi.org/10.1177/09544097221122036

DIPARTIMENTO DI MECCANICA ■ POLITECNICO DI MILANO
via G. La Masa, 1 ■ 20156 Milano ■ EMAIL (PEC): pecmecc@cert.polimi.it
http://www.mecc.polimi.it
Rev. 0

Experimental characterization of the vibration effects on wheels of a mass rapid transit vehicle

L. Calvanese[1[0000-0002-9777-7347]], E. Di Gialleonardo[1[0000-0003-1393-2942]], M. Bocciolone[1[0000-0002-2546-6486]]

[1]Dipartimento di Meccanica, Politecnico di Milano

Milan, Italy

Declarations

Funding

Not applicable

Conflicts of interest/Competing interests

The authors declare that they have no conflict of interest.

Availability of data and material

Not applicable

Code availability

Not applicable

Authors' contributions

L. Calvanese: Investigation, Methodology, Data curation, Writing - original draft, Writing - review & editing.

E. Di Gialleonardo: Investigation, Methodology, Data curation, Writing - review & editing.

M. Bocciolone: Investigation, Methodology, Writing - review & editing.

Abstract

The aim of this paper is to present the results coming from an experimental campaign aimed at the definition of the vibrations acting on a powered and a trailer bogie of a railway vehicle for mass rapid transit during commercial service. The results, coming from multiple sensors placed in specific points of the two wheelsets, can give a significative overview of the dynamic behaviour of the two components, highlighting, when present, notable differences. The available sensors gave the possibility to justify and correlate these differences to specific characteristics of the bogies considered. The study stresses the presence of peculiar cyclic solicitations that the wheels and the wheelset undergo during their service. A deeper investigation of the outcoming signals has been carried out keeping into consideration the frequency content associated to the specific measurement system in use. The results of the experimental campaign highlight that powered wheelsets may experience significant high-frequency vibrations induced by gear pairs. The implications of these findings may represent a significant argumentation in the discussion of the design requirements of wheelsets and wheels.

Introduction

Railway bogie and axle design requires a deep knowledge of the static and dynamic loading acting on mechanical components during commercial service. International

standards designated to this scope define all the loading conditions that must be kept into account when designing a new bogie frame or an axle.

Focusing the attention on powered axles equipped with monobloc wheels, Standards EN 13103[1] and DD CEN/TS 13979[2] define the procedures needed for the assessment of fatigue life respectively of the non-powered and powered axles and the wheels.

Following the standards, the loading conditions for the design of the components does not directly consider dynamic effects, considering quasi-static forces due to masses in motion, traction, braking and curving. As a drawback some peculiar dynamic loading conditions are ignored in the design phase of the components.

To have a clear overview of the loads a railway vehicle undergoes during the commercial service, an experimental campaign has been set up. The main scopes are the definition of the frequency contents of the contact forces acting between the wheels and the rail and a preliminary estimation of the axle fatigue stresses. To do that, a peculiar measurement setup has been adopted. A first setup was directly aimed at the measurement of the contact forces acting on the wheels of a trailer bogie of the railway vehicle under study. This setup was applied only to the trailer bogie due to the lack of available space on the powered one.

Moreover, to have information about the effect the traction system has on the bogie behaviour, a powered and a trailer bogie have been instrumented with a series of strain

gauges measuring the deformations in correspondence of the wheels. Due to the direct relationship between the contact forces and the wheels' deformations, these strain sensors give the possibility to evaluate possible differences in the solicitation state of the powered and the trailer bogie. In the end additional sensors were applied to the already instrumented bogies, two triaxial accelerometers were placed in correspondence of the axleboxes. This auxiliary system guaranteed the visibility of high frequency dynamical effects which can be induced by the traction system (gearbox and motor), due to the higher sampling frequency allowed by the acquisition system.

Many studies concerning gearbox dynamic effect on the wheelset have been performed in recent years. References[3–7] focus their attention on the gearbox fault diagnosis, the main objective is to identify gearbox defects like gear tooth cracks. To do that, these works propose different solutions, like the wavelet analysis of the vibrations induced by the defects, or the analysis of the torsional vibrations. Other works like [8–11] investigate the gearbox housing deformations and stresses during the vehicle service through the development of multibody models or peculiar measuring setups. Their objective is the evaluation of the fatigue life of the housing itself and the possible risks associated to cracks opening and propagation. Other works like [12–16] are aimed at the analysis of the impact the traction system and the gear mesh frequencies can have on the overall dynamic of the vehicle.

The aim of this paper is to present a frequency characterization of the vibrations acting on a railway vehicle and strengthen the importance of considering high-frequency stresses that may arise due to the presence of the gearbox on a powered wheelset, not only in high-speed applications. In fact, the results of the experimental campaign presented in the paper will prove that, apart from traction forces, the stresses due to low frequency dynamics of the vehicle on trailer and powered wheelsets are very similar. Important differences, on the other hand, are found on high frequency components that are triggered by the presence of gear pairs.

The implications of the results on fatigue stresses could be of high interest mostly for the definition of new standards in the design and maintenance of powered axles. In fact, the clear definition of the stresses acting on the wheelset components is fundamental for the calculus of the fatigue life of the wheels and the axle[17]. Moreover, in the trending research framework of fatigue assessment of wheels due to rolling contact fatigue [18–20], this work could increase the information related to wheel solicitation.

In the following paragraphs, at first a description of the experimental setup employed in the tests is provided, presenting the different measuring systems adopted during the test campaign; then the results of the experimental campaign are presented and discussed with proper analyses in the time and the frequency domains, highlighting, when present, the differences between the motor and the trailer bogie axles. Finally, some concluding remarks are provided.

Experimental set-up

In this section the experimental setup mounted on a train for mass rapid transit is described. The vehicle is a six-car train, with four powered cars and two trailer ones. A number of sensors have been applied to two axles, respectively belonging to a trailer and a motor bogie of the vehicle.

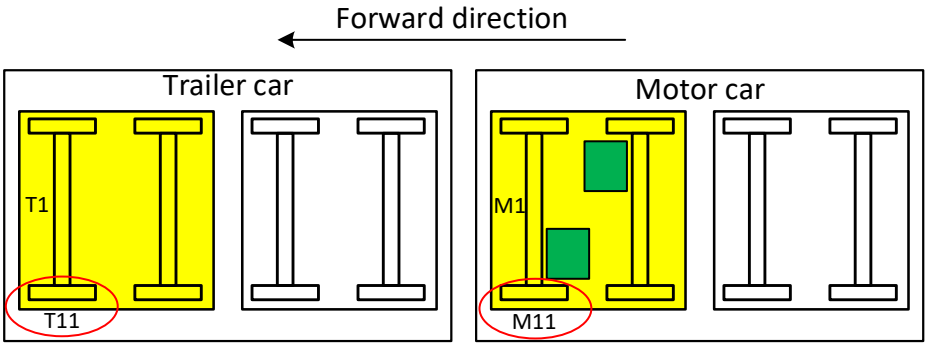

Fig 1 Simplified scheme of the instrumented bogies

To study the stresses that characterize the vehicle wheelset under commercial loading conditions, different systems of measure were adopted. The first measuring setup employed in this study is a contact force measuring system (mounted on wheelset T1 in Fig 1) already successfully applied in previous works, the so-called instrumented

wheelset presented in detail in other studies[21]. The contact forces acting on both wheels are extrapolated from a proper calibration of a series of strain gauges placed on the axle and the wheels. In the specific application, on account of the reduced space for allocating the strain gauges on the spindles, the elongation of the primary suspension was also considered in the measurement set, as explained in details in another work[22].The measurements are performed estimating three components for each wheel-rail contact force: the vertical, the lateral, and the longitudinal one. The vertical and lateral loads can be associated to the bending deformation of the axle in the vertical plane, the longitudinal component, instead, is mainly responsible for the torsional deformation of the axle. Given these information, the calibration is performed considering an overabundant number of sensors with respect to the six unknowns, in such a way to increase the accuracy of the overall estimation. The wheelset is used as a measurement device, under the hypothesis of a linear relationship between the applied loads and the resulting strains. Of course, this assumption is valid only in the quasistatic region, so well below the location of the deformable modes of the axle. This limits the bandwidth of the instrumented wheelset approximately up to 40 Hz. Since the available space on the motored axle was not sufficient, this system was designed and applied only on the axle of the trailer bogie. Thanks to this system an idea of the contact forces acting on both wheels of the trailer bogie are acquired and analysed in the following paragraphs. The results obtained with this setup can be considered representative also of what happens on the motored axle

except for the traction stresses. These stresses can be easily quantified in the quasi-static region and added to the data obtained from the trailer bogie.

The second setup is the one aimed at measuring the strains on a single wheel for each instrumented axle, denoted respectively as T11 and M11 in Fig 1.

This has been performed using strain gauges applied to different points of the wheel, as shown in Fig 2. Before making explicit the positions of the strain gauges over the instrumented wheels it results necessary specifying that the wheels considered in this application presented a series of small holes over a circumference at the extremity of the wheel profile. These holes were aimed at the optional installation of the wheel damper system, typically employed for the reduction of rolling and squeal noise[23], not mounted on the wheels in the final in-service configuration. For this reason, when considering the location of the strain gauges on the wheel, the presence of the holes played a significant role in the decision due to the stress intensification. After this short preamble, the position of strain gauges is schematically represented in Fig 2.

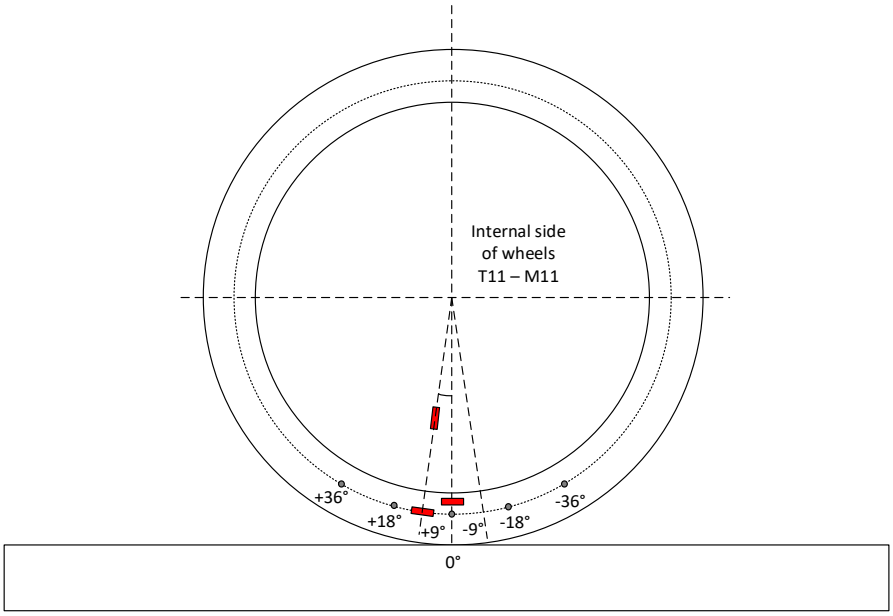

Fig 2 Schematic representation of strain gauges position on the wheel

One sensor is placed on the wheel web measuring the radial strain. As will be demonstrated, this sensor is highly sensitive to the lateral component of the contact force. The other two measure the circumferential strain respectively in correspondence of a hole and between two holes. The configuration of each Wheatstone bridge is quarter bridge. The conditioning of the strain gauge is performed by a specific module (mounted on the wheel) that is also making the A-D conversion. The data are then transferred by means of a wireless transmitter from the rotating system to a non-rotating receiver mounted on the carbody. The technical characteristics of the wireless systems limit the sampling frequency of each channel to 256 Hz.

To understand the effects of the contact force between the wheel and the rail on the measure of the strain gauges as a function of their different positions, some tests have been performed. The tests have been carried out using the same dedicated test-rig specifically designed for the calibration of the instrumented wheelset, previously described.

These tests consisted in the measurements of the resulting strain coming from the application of different combinations of vertical and lateral forces on the wheels. Fig 3 shows the results of a set of these tests. In the figure, the measured strains are plotted as function of the vertical loads (plots in the left column) and of the lateral loads (plots in the right column). Analysing the diagrams, the first thing that catches the eye is that the wheel web sensor (top plots) is the most sensitive to the lateral load amplitude with respect to the other two sensors locations. More in detail, it appears that the radial strain measured at the wheel web is linearly dependent from the lateral load magnitude. All the other measurements do not bring to such clear conclusions, even if a direct proportionality between the strains and the load amplitudes is always present. As a conclusion statement it can be affirmed that the two sensors placed in correspondence of the holes, measuring the circumferential strains, are subjected to a more complex stress distribution with respect to the sensor placed at the wheel web, which instead, is mainly affected by the wheel bending strain distribution. Consequently, its measure can be mostly associated to the lateral excitation of the wheel. On the other hand, the strain gauges placed in

correspondence of the holes give information about the resulting stresses due to the combined application of lateral and vertical loads on the wheel.

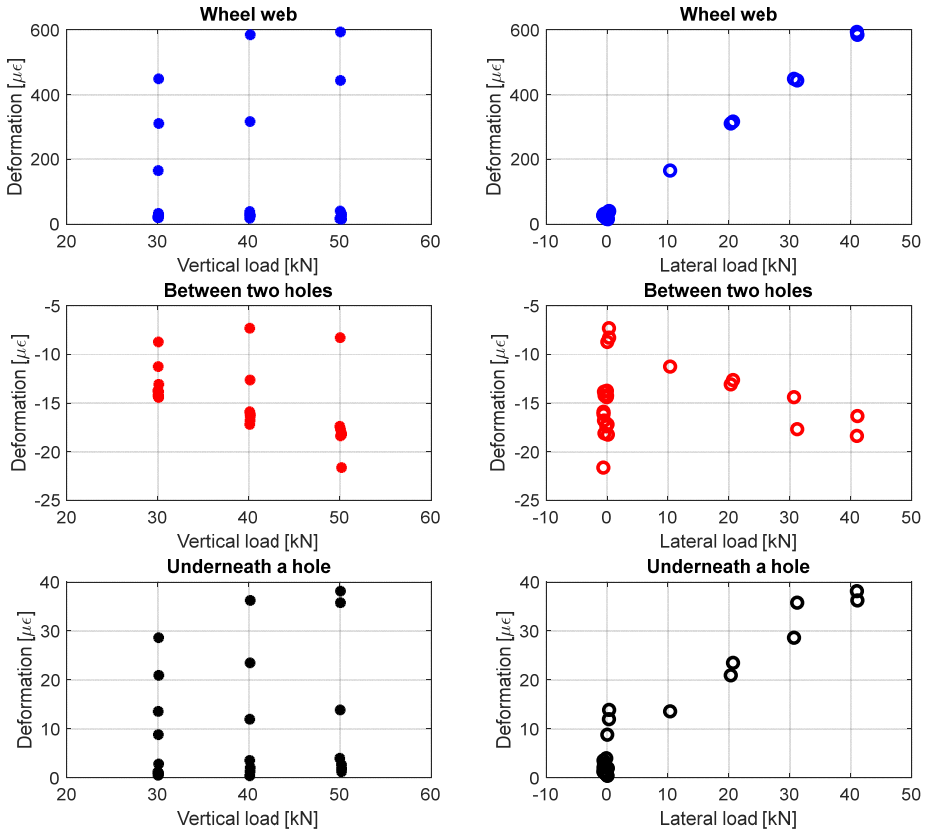

Fig 3 Strain measurements obtained for different values of the vertical force (left column) and lateral force (right column) in correspondence of the wheel web (top plots), between two holes (middle plots) and underneath a hole (bottom plots)

The last setup employed in the experimental campaign aims at the investigation of the high-frequency dynamics of the system. This is obtained through a set of triaxial accelerometers installed on different locations on the non-rotating components of the vehicle. This permits to avoid telemetry systems thus increasing the maximum sampling frequency. Accelerometers have been installed in correspondence of the axleboxes, both for the trailer bogie and the motor one (as shown in Fig 1), and on the gearbox housing of the powered axle M1. The data acquisition system adopts a sampling frequency of 2048 Hz. Thus, the acquired signals include the high frequency of the vehicle components, as for example the contribution of the bending modes of the wheelset. Other relevant sensors were employed and, for sake of brevity, are not described here in details, e.g., the odometry system and additional sensors aimed at the localisation of the vehicle along the railway line.

Results of the experimental campaign

An experimental campaign was designed ad hoc for taking out the vehicle from the service and carrying out special runs with the train travelling through its commercial route. Tests have been performed in different vehicle load conditions, however, for the sake of brevity only the exceptional load condition (considering the presence of 6 passengers/m^2) will be analysed. The route, that is approximately 16 km long, includes several curves with different radii, whose distribution is reported in Table 1 (the class

with curve radius larger than 3000 m also includes straight track sections), acceleration and braking transients. This, together with the fact that the track presents different levels of geometrical defects (longitudinal level, alignment, twist, presence of insulated joints, …), determine running conditions representative of the life cycle of the vehicle. Hereafter, the results of the experimental campaign are analysed in time and in frequency domains.

Curve radius [m]	R > 3000	1200 ≤ R < 3000	900 ≤ R < 1200	600 ≤ R < 900	300 ≤ R < 600	R < 300
Occurrence [%]	59.4	4.7	3.5	6.1	11.2	15.1

Table 1: distribution of curve radii along the considered route.

In the following the results of the three measuring systems, described in the previous section, will be presented. First, the contact forces on the trailer wheelset will be shown in order to verify that they are in typical range for mass rapid transit vehicle. This is important since actual standards for wheel and axle design are based on maximum values of these quantities. Secondly, strain measurements on both powered and trailer wheelsets will be presented comparing the dynamic components of the wheel stresses. Lastly, acceleration measurements on the wheelsets will be compared in order to understand the differences induced by high-frequency phenomena.

It is worth remarking that the three measuring systems have different bandwidths: the instrumented wheelset can be used to estimate the contact forces up to 40 Hz; the frequency range of strain measurements on the wheels is limited to approximately 100 Hz on account of the bandwidth of the wireless transmission, finally the accelerometer system can measure frequency contents up to around 800 Hz.

Force measurements

In this paragraph the results of the estimation of the contact forces performed by the instrumented wheelset are discussed. It is important to keep into consideration that, as already said in section 2, the wheel-rail contact forces are measured only on the trailer axle T1.

A rainflow analysis is performed on the vertical and lateral components of the wheel-rail contact force. To extract a single value for each load cycle, the maximum load value is collected, defined as the sum of the mean value and the amplitude of the cycle. Histograms of the occurrences of the maximum values for the vertical and lateral contact forces acting on wheel T11 are shown in Fig 4. As far as the vertical component is concerned (Fig 4 left), the values are almost symmetrically distributed around a mean value (approximately equal to 52 kN). This is coherent with straight track negotiation and the load transfer in curves, assuming that a homogenous distribution of left and right hand curves (T11 is assumed to be alternatively the inner and outer wheel) is present along the

route. Defects on track geometry superimposes a dynamic on the quasistatic behaviour defined by the track layout and the vehicle speed.

On the other hand, considering the lateral component of the contact force the histogram (shown in Fig 4 right) highlights that the most frequent value is around zero. Again, this is coherent with the fact that in straight track the lateral force acting on the wheel is quite small, while the negotiation of the curves is responsible for the high values especially when the considered wheel is acting as the guiding one.

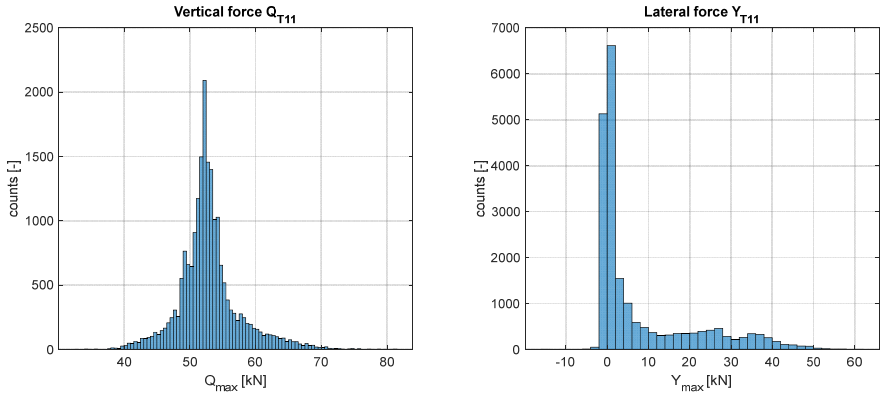

Fig 4 Histogram of the occurrences of the maximum value of the vertical (left plot) and lateral (right plot) component of the contact force acting on wheel T11

Strain measurements

To extend the considerations on the load spectra obtained in the previous subsection to the powered wheelset, it is possible to take advantage of the comparison between strain

measurements on the homologous wheels T11 and M11. In fact, it is worth noticing that the suspension elements are the same for the trailer and motor bogies, which should imply a very similar bogie attitude in curve negotiation. Therefore, the only difference between the two is the presence of the traction system. This leads to a change in the unsuspended masses and to the introduction of high-frequency dynamical components due to the motor and the gearbox.

In section 2 it was proved that the wheel web radial deformation can be used for inferring the lateral load, thus, if present, this signal should highlight possible differences in the behaviour of the two bogies, in the frequency range investigable by the considered measurement system.

As an example, the results of the rainflow analysis carried for the wheel-web strain measure is reported in Fig 5. The diagram represents the counts as a function of the rainflow cycles. The comparison between the trailer (T11) and motor (M11) wheels highlights that the stresses induced by the lateral component of the contact force is analogous.

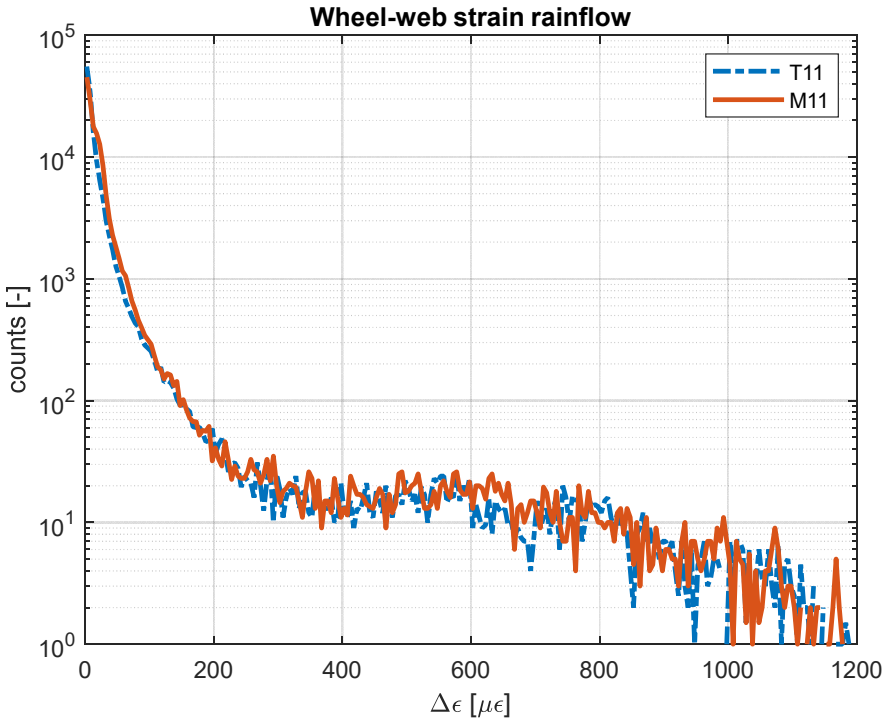

Fig 5 Rainflow analysis of the wheel-web strain on trailer T11 and motor M11 wheels

On the other hand, Fig 6 shows the comparison between the power spectral densities (PSD) of the strain signals coming from the sensors place underneath the holes of the two wheels T11 and M11. The main frequencies are almost superimposed. These strain measurements are not only representative of the lateral excitation acting on the wheel, as those coming from the wheel web sensors, but as already mentioned in section 2, should account for a more complex stress distribution sum of different contributions. For this reason, this plot gives a more general indication, with respect to Fig 5, on the comparison

between the trailer and motor wheels, highlighting that, even considering a superimposition of stresses, the dynamics of the trailer and motor wheels are almost equal.

These evaluations can be retained valid up to 100 Hz approximately which is the bandwidth of the considered measurement system.

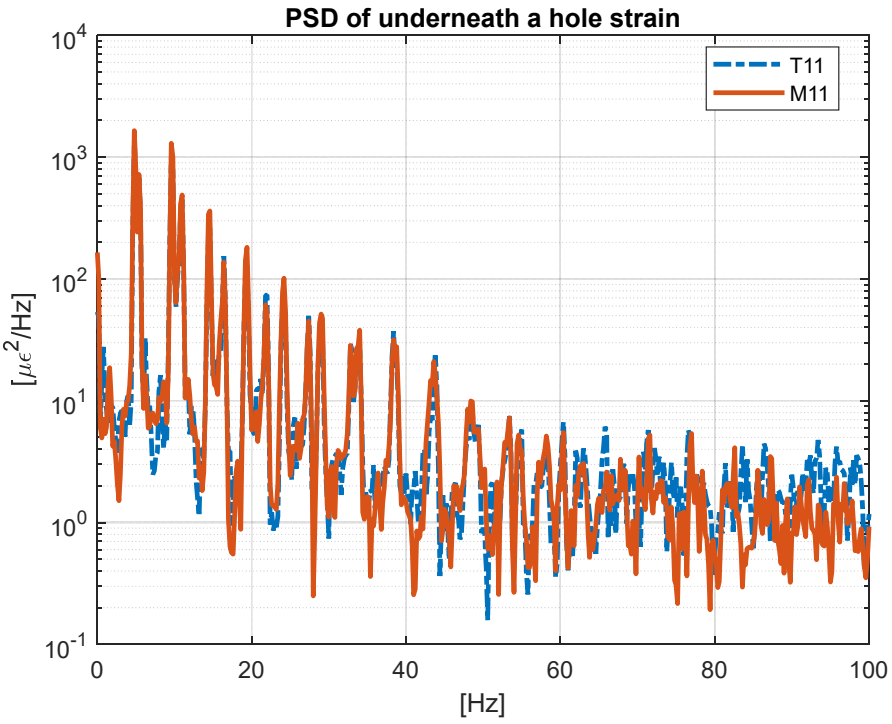

Fig 6 Comparison in logarithmic scale (vertical axes) of the PSD of the circumferential strain measured by the sensors place underneath the holes of wheels M11 and T11

Acceleration measurements

Different indications can be extracted from the acceleration signals of the auxiliary measurement setup. As can be seen in the bottom plot of Fig 7, the vertical accelerations measured at the two axleboxes are of the same order of magnitude for most of the time. Higher values are alternating on both axles, but always reaching reciprocally comparable magnitudes. Lateral accelerations, instead, depicted at the top of Fig 7, differ significantly passing from an axle to the other. In a large portion of the time histories, the lateral acceleration measured in correspondence of the wheel M11 of the motor bogie axle is almost an order of magnitude higher with respect to the one in correspondence of the wheel T11 of the trailer bogie axle. This appears strange, considering that until now no significative difference was found between the two axles behaviour.

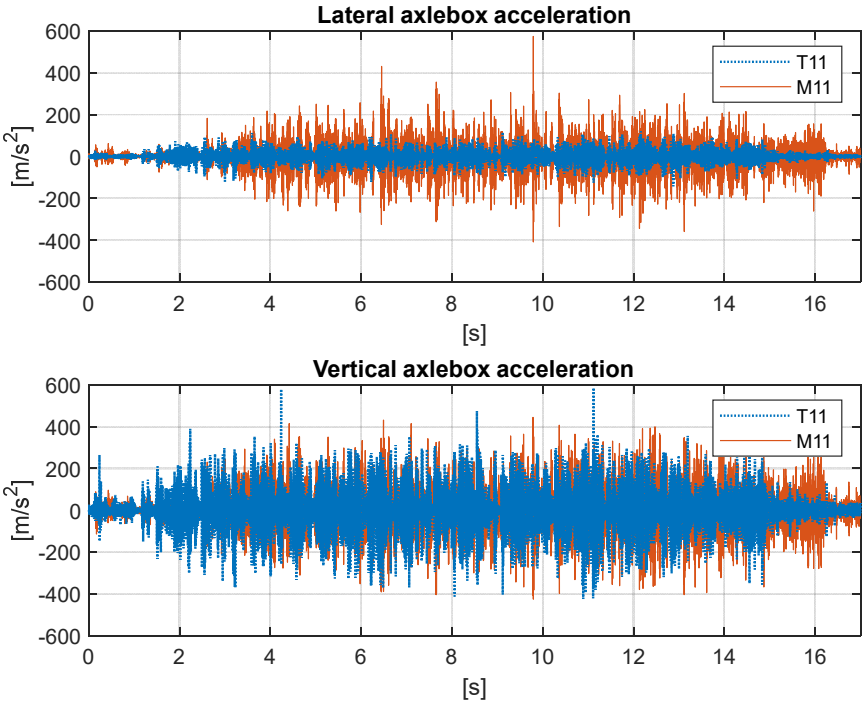

Fig 7 Acceleration measurements comparison between the accelerometers on the axlebox in correspondence of wheel M11 and wheel T11. On the top the vertical accelerations are depicted, instead, on the bottom the lateral accelerations are shown

The plot of the PSD of the lateral accelerations of Fig 8 identifies a large difference in the frequency content of the signals at frequencies higher than 200 Hz. From an overview of the performed tests, it resulted that this difference is more accentuated in correspondence of curve negotiations. It is probably favoured by the variation in the constraint condition caused by these manoeuvres.

Due to the very similar structure of trailer and motor bogies, this difference must be mainly attributed to the presence of the motor and gearbox on the motor bogie axle.

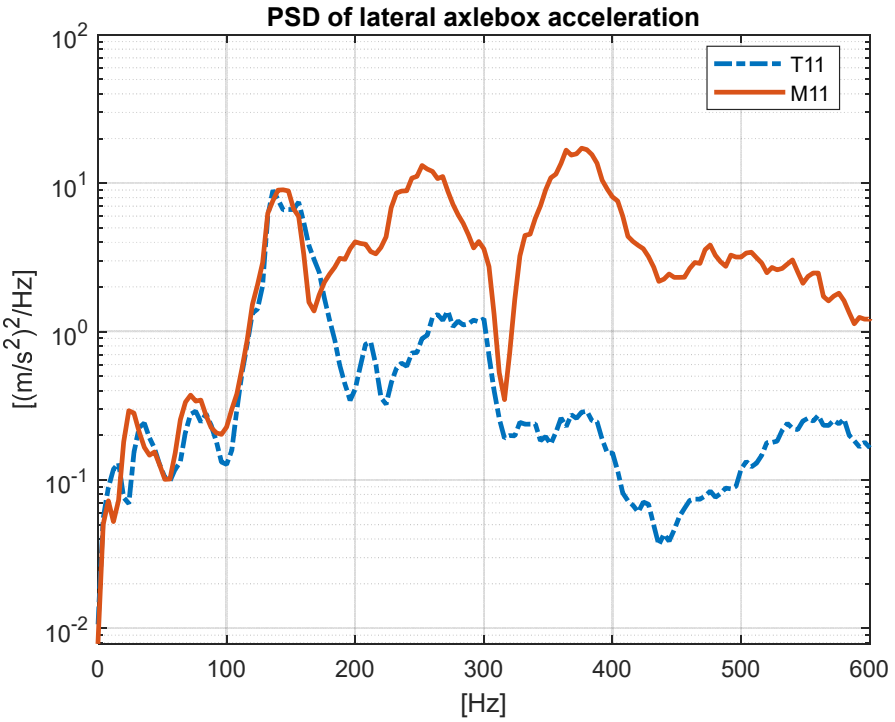

Fig 8 Comparison in logarithmic scale (vertical axes) of the PSD of the lateral accelerations in correspondence of the two wheels T11 and M11

Discussion

In this section, some remarks about the results obtained in the experimental campaign are presented.

With regard to the solicitations acting on the trailer bogie, these has not presented criticalities. The analysis of the contact force components acting on the wheel T11, in the frequency bandwidth of the system of measure, is coherent with the tests characteristics. The analysis of the strains measured at the two wheels T11 and M11 confirmed that the indications obtained for the trailer bogie were valid also for the motor one. In addition to this, the strain measuring system confirmed the idea that the dynamics of the two bogies are comparable, this is true until the limiting frequency of 100 Hz, as shown in Fig 5 and Fig 6.

The acceleration measuring setup, instead, highlighted significative differences between the trailer and motor bogies.

The fact that the differences encountered in the acceleration signals analysis (Fig 7) are not visible in the strain signals highlights the presence of an excitation source at a frequency higher than the Nyquist frequency of the strain acquisition system, as confirmed by the PSD shown in Fig 8.

At first, no obvious evidence was found behind this difference. Especially if considering the two axles test environment. The motor and trailer axles both passed through the same

route and apparently underwent the same external excitations. The reason behind this high frequency different dynamic behaviour must be sought in the additional components the motored bogie is equipped with. In particular, the origin can be attributed to the gear mesh frequency excitation of the gearbox mounted on the motor axle.

To deepen the correlation between the acceleration difference encountered comparing the lateral accelerations of the motor and trailer axle, it is necessary to study the gearbox characteristics, highlighting the gear mesh frequencies with the help of some numbers. In this specific application, the vehicle motor speed is reduced by means of two stages. Among the mesh frequencies generated by the gearbox gear couplings, the lowest is associated to the output of the second stage, which is characterized by the lowest rotating speed. Since the output of the second stage is the rotating speed of the wheels, this frequency can be directly related to the vehicle speed and evaluated with the following expression[13]:

$$f_c = \frac{V * N_t}{\pi * D}$$

Where V is the vehicle speed, N_t is the number of the considered gear's teeth and D is the wheel diameter. Substituting in Equation 1 the commercial speed range of the vehicle considered (ΔV_{sample} = 30-70 km/h), the number of teeth of the slower gear of the second stage, which is equal to 59 and the nominal diameter of the vehicle wheels ($D_{nominal}$ = 0,82 m), the frequency range obtained is 190-445 Hz. This result is in good accordance with

the indications obtained looking at the plot of Fig 8. Fig 9 shows the PSD of the lateral acceleration measured by the accelerometer placed on the gearbox housing. In this plot is clearly visible a high frequency content of the signal between 200 and 400 Hz, this appears coherent with the gear mesh frequency range calculation just performed.

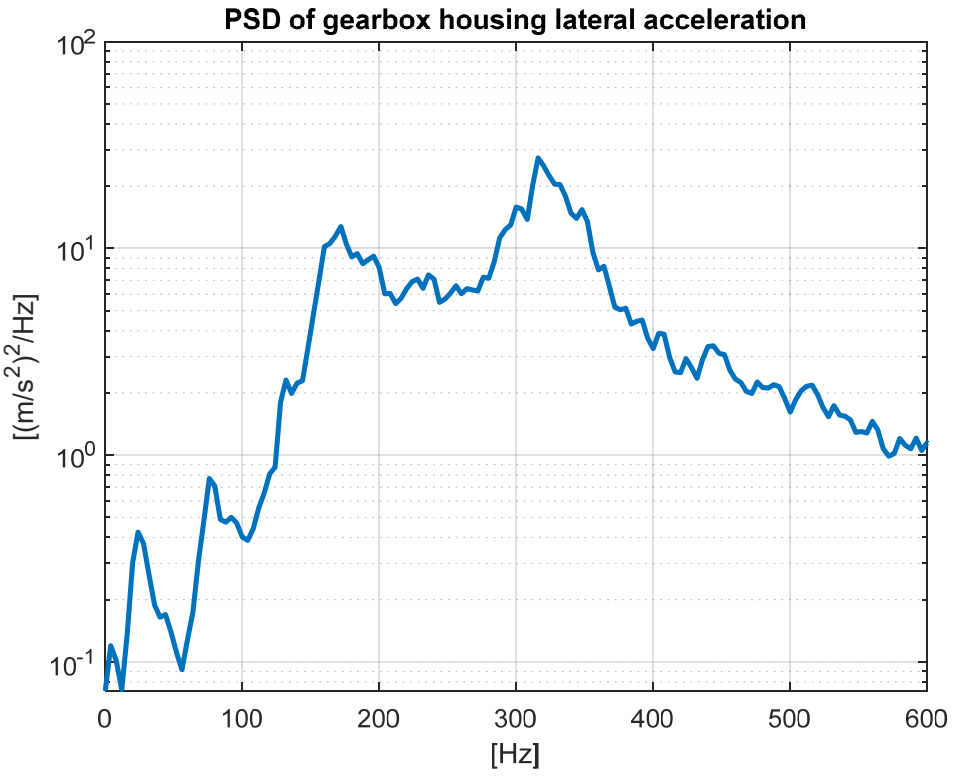

Fig 9 PSD of the lateral acceleration measured in correspondence of the gearbox housing

This excitation can be associated to the frequency content of a load, mainly generated by the vibration of the gearbox, able to excite the vibrating modes of the motor axle. This assumption is strengthened by the two plots of Fig 10. The two plots show two frequency

response functions extrapolated from impact tests performed on a trailer wheelset. For the same input, a hammer vertical impact on the axle, the two FRFs are obtained considering as output a vertical acceleration measured on a wheel, top plot, and a lateral acceleration measured on the same wheel, bottom plot. The impact tests considered the wheelset as suspended, so, its dynamic behaviour during commercial service can partially differ from the one shown in the two plots.

It is assumed that trailer and motor wheelset are represented by similar FRFs (the wheelset and wheels dimensions are approximately the same), it is expectable that the plots of Fig 10, neglecting some small differences, are representative of both axles.

So, the different magnitude of the lateral vibrations of the motored axle resides in the fact that its resonant frequencies, in the 200-400 Hz range, are excited by the gearbox presence. Thus, the resonant response of the wheelset to the excitation produced by the gearbox, justifies the higher values of the lateral accelerations clearly visible in the comparison between the motor and trailer axle of Fig 8.

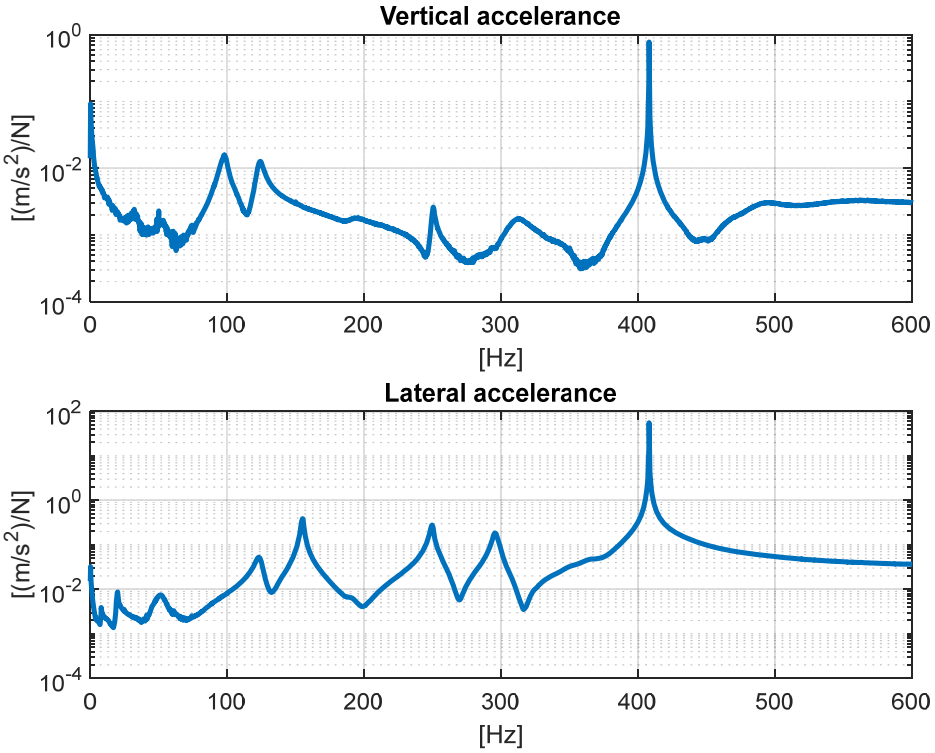

Fig 10 Frequency response functions obtained exciting a vehicle wheelset with impact hammer. The FRFs are obtained measuring the vertical (top plot) and the lateral (bottom plot) accelerations generated by a vertical impact

High cycle fatigue considerations

Without having the claim of assessing the fatigue resistance of the wheelset under the complex dynamic stress distribution, the objective here is to make a simple evaluation of the possible risks that this high frequency excitations could cause with respect to the

nominal stresses the wheelset is designed for. Due to the presence of the gearbox excitation, a life reduction of the wheelset components, which undergo this cyclic stress, could occur. In general, apart from the axle itself, one of the most stressed components are the wheels. In the wheels the axle lateral vibration, highlighted in this work, sums with the rotating bending and torsional (due to traction and/or braking actions) stress distributions. The excitation given by the gearbox vibration can be traduced in a cyclic load. If the vehicle speed tunes the gear mesh frequency with one of the wheelset eigenfrequencies for most of the commercial service, the risk is that the wheels perform, in few service routes completion, a very high number of cycles under the excitation of the gearbox. An increasing risk is given by the presence, in some wheels profile like the ones tested during the experimental campaign at the base of this paper, of small holes in correspondence of the wheels' extremities. The stress concentration effects caused by these surface carvings, could cause a significant reduction of the material fatigue resistance. In the worst scenario this fatigue resistance reduction could bring very low amplitudes vibrations to cause cracks initiation starting from corrosion inside these holes or from small surface damages.

Conclusions

What has been presented in the previous sections of this paper brings to interesting conclusions. Even if the trailer and the powered wheelsets present a very similar dynamic

behaviour at low frequencies, significative differences arise when the analysis moves to high frequencies. The different setups employed in the analysis, , have given back interesting results. On one hand, the strain and force measurements demonstrated that until the 100 Hz limit the behaviour of the trailer and motored bogies are comparable and do not present any anomaly. On the other hand, the acceleration setup shows the impact of the peculiar excitation acting on the powered axle. This effect is visible only in the signals coming from this setup due to the higher sampling frequency involved which can capture the axles high-frequency dynamics. The post processing of the acceleration signals allowed to associate this vibration to a frequency range, between 200 and 400 Hz. Looking at the frequency response functions of the wheelset, it resulted that this frequency range is close to one of the main wheelsets eigenfrequencies and it contains additional resonances.

As discussed, the gearbox generates vibrations associated to gears meshing. This fact gains a harmful relevance when the vehicle speed allows one of the gear mesh frequencies to equal one of the vibrational modes of the wheelset. A simplified calculus confirmed that the gear mesh frequency range considering the commercial speeds of the vehicle covers the 200-400 Hz range.

As a general comment, further investigations are needed in order to acquire more information regarding the amplitude and the effects of the related mechanical stress. In fact, the extremely high number of cycles, supported by the high frequency at stake,

makes it necessary to evaluate the potential fatigue life reduction of the components involved.

Moreover, it would be interesting to investigate the possible correlation between the rail route characteristics, like curves and defects, and this gearbox excitation. The application of a strain measurement system able to effectively detect the high frequency excitation explored in this work would give the chance to measure the effective strain on the wheels, and the correspondent stresses, leading to a more precise and complete analysis of the structural risks.

The main outcome of the present research may represent a warning for railway engineers. In fact, as shown in the paper. gearbox induced vibrations may lead to unexpected stresses on safety components of the vehicle, that may affect their fatigue resistance. From the operational point of view, an evaluation on the mean service speed can be assessed in order to avoid the frequency tuning of gear mesh frequencies with the eigenmodes of the wheelsets for most part of the commercial route.

References

1. British Standards Institution. BS EN 13103-1 : 2017 Railway applications - Wheelsets and bogies.

2. DD CEN/TS 13979-2:2011. Railway applications. Wheelsets and bogies. Monobloc wheels. Technical approval procedure. Cast wheels.

3. Henao H, Kia SH, Capolino GA. Torsional-vibration assessment and gear-fault diagnosis in railway traction system. *IEEE Trans Ind Electron* 2011; 58: 1707–1717.

4. Lin J, Zuo MJ. Gearbox fault diagnosis using adaptive wavelet filter. *Mech Syst Signal Process* 2003; 17: 1259–1269.

5. Wang W. Early detection of gear tooth cracking using the resonance demodulation technique. *Mech Syst Signal Process* 2001; 15: 887–903.

6. Cai Y, He Y, Li A, et al. RETRACTED ARTICLE: Application of wavelet to gearbox vibration signals for fault detection. *Proc - 2nd IEEE Int Conf Adv Comput Control ICACC 2010* 2010; 4: 441–444.

7. Feng Z, Zuo MJ. Vibration signal models for fault diagnosis of planetary gearboxes. *J Sound Vib* 2012; 331: 4919–4939.

8. Wu H, Wu P, Xu K, et al. Research on Vibration Characteristics and Stress

Analysis of Gearbox Housing in High-Speed Trains. *IEEE Access* 2019; 7: 102508–102518.

9. Hu W, Liu Z, Liu D, et al. Fatigue failure analysis of high speed train gearbox housings. *Eng Fail Anal* 2017; 73: 57–71.

10. Bartelmus W, Zimroz R. A new feature for monitoring the condition of gearboxes in nonstationary operating conditions. *Mech Syst Signal Process* 2009; 23: 1528-1534.

11. Kumar A, Jaiswal H, Jain R, Patil P, Free vibration and material mechanical properties influence based frequency and mode shape analysis of transmission gearbox casing, *Procedia Engineering* 2014; 97: 1097-1106,

12. Zhang T, Chen Z, Zhai W, et al. Establishment and validation of a locomotive–track coupled spatial dynamics model considering dynamic effect of gear transmissions. *Mech Syst Signal Process* 2019; 119: 328–345.

13. Ren Z, Xin X, Sun G, et al. The effect of gear meshing on the high-speed vehicle dynamics. *Veh Syst Dyn*. Epub ahead of print 2020. DOI: 10.1080/00423114.2020.1711955.

14. Chen Z, Zhai W, Wang K. Locomotive dynamic performance under traction/braking conditions considering effect of gear transmissions. *Veh Syst Dyn*

2018; 56: 1097–1117.

15. Huang GH, Zhou N, Zhang WH. Effect of internal dynamic excitation of the traction system on the dynamic behavior of a high-speed train. *Proc Inst Mech Eng Part F J Rail Rapid Transit* 2016; 230: 1899–1907.

16. Feng Z, Xiao H. Analysis of Stability and Vibration Transmission Law of Type A Metro Vehicles. *J Phys Conf Ser*; 1846. Epub ahead of print 2021. DOI: 10.1088/1742-6596/1846/1/012029.

17. Zerbst U, Mädler K, Hintze H. Fracture mechanics in railway applications - An overview. *Eng Fract Mech* 2005; 72: 163–194.

18. Ekberg A, Kabo E, Lundén R, et al. Stress gradient effects in surface initiated rolling contact fatigue of rails and wheels. *Wear* 2016; 366–367: 188–193.

19. Lundén R, Vernersson T, Ekberg A. Railway axle design: To be based on fatigue initiation or crack propagation? *Proc Inst Mech Eng Part F J Rail Rapid Transit* 2010; 224: 445–453.

20. Zhao X, Wang Z, Wen Z, et al. The initiation of local rolling contact fatigue on railway wheels: An experimental study. *Int J Fatigue* 2020; 132: 105354.

21. Cazzulani G, Di Gialleonardo E, Bionda S, et al. A new approach for the evaluation and the improvement of the metrological characteristics of an instrumented

wheelset for the measure of wheel-rail contact forces. *Proc Inst Mech Eng Part F J Rail Rapid Transit* 2017; 231: 381–393.

22. Bionda S, Di Gialleonardo E, Crosio P, et al. Integration of the measure of the primary suspension deflection into a dynamometric wheel-set equipped with strain gauge bridges. In: *Proceedings of the Mini Conference on Vehicle System Dynamics, Identification and Anomalies*. 2014, pp. 243–252.

23. Knothe K, Stichel S. Determination of Load Collectives for Vehicle Components. In: *Rail Vehicle Dynamics*. Cham: Springer International Publishing, pp. 273–295.